Transcriptomic analysis of lipoteichoic acid-treated undifferentiated and neutrophil-like differentiated HL-60 cells

KUAN-TING LIU[1,2], I-JENG YEH[1,3], YA-LING HSU[4] and MENG-CHI YEN[1,3]

[1]Department of Emergency Medicine, Kaohsiung Medical University Hospital; [2]School of Medicine; [3]Graduate Institute of Clinical Medicine; [4]Graduate Institute of Medicine, College of Medicine, Kaohsiung Medical University, Kaohsiung 80708, Taiwan, R.O.C.

Received August 18, 2023; Accepted January 18, 2024

DOI: 10.3892/etm.2024.12446

Abstract. Toll-like receptor 2 (TLR2) is an important sensor for innate immune cells, including neutrophils, for the recognition of pathogen infection. Lipoteichoic acid (LTA), a cell wall component of gram-positive bacteria, is a TLR2 ligand. LTA-induced TLR2 signaling pathways are well established in neutrophils. However, experimental studies regarding transcriptional regulation and the molecular mechanisms in primary human neutrophils are limited due to their short lifespan. The promyelocytic leukemia cell line, HL-60, can differentiate into a neutrophil-like phenotype following treatment with dimethyl sulfoxide. The aim of the present study was to investigate whether differentiated HL-60 (dHL-60) cells induced a similar gene expression profile upon LTA treatment as that previously determined for primary human neutrophils. After 4 or 24 h of *Staphylococcus aureus* LTA treatment, undifferentiated HL-60 (uHL-60) and dHL-60 cells were collected for RNA sequencing. The results demonstrated that hundreds of identical differentially expressed genes (DEGs) were observed in 1 and 10 μg/ml LTA-treated dHL-60 cells following 4 and 24 h of incubation, while almost no DEGs between LTA-treated HL-60 and dHL-60 cells were observed. Using Gene Ontology (GO) and Kyoto Encyclopedia of Genes and Genomes analyses (KEGG), it was noted that the pathways of shared DEGs between the 1 and 10 μg/ml LTA-treated dHL-60 cells at both time points were significantly enriched in immune and inflammatory response-related pathways, such as cellular response to tumor necrosis factor, interleukin-1, interferon γ, neutrophil chemotaxis, the NF-κB signaling pathway and the Toll-like receptor signaling pathway. In addition, when comparing the effect of 1 and 10 μg/ml LTA treatment on dHL60 cells, it was found that all enriched GO and KEGG pathways were associated with the TLR signaling pathways of neutrophils. The results of the present study provided important information for the implementation of mRNA profiling in LTA-treated dHL-60 cells and may indicate the feasibility of using dHL-60 cells as a research model for TLR2 signaling in human neutrophils.

Correspondence to: Dr Meng-Chi Yen, Department of Emergency Medicine, Kaohsiung Medical University Hospital, Kaohsiung Medical University, 100 Shih-Chuan 1st Road, Sanmin, Kaohsiung 80708, Taiwan, R.O.C.
E-mail: yohoco@gmail.com

Key words: HL-60, neutrophil, differentiation, lipoteichoic acid, RNA sequencing, transcriptomic analysis

Introduction

Neutrophils constitute 50-70% of white blood cells in humans (1), and are short-lived effector cells of the innate immune system that play an important role in the response to extracellular pathogens (2). These pathogens can be recognized by pattern recognition receptors on neutrophils, which subsequently activate anti-pathogen responses, including the production of reactive oxidative species (ROS) and inflammatory mediators, the release of lytic enzymes from granules and the formation of neutrophil extracellular traps (NETs) (3-5). The toll-like receptor (TLR) family is a class of pattern recognition receptors (6). With the exception of TLR3, all TLRs are expressed in neutrophils (7). The TLR family plays a critical role in innate bacterial recognition (8). For example, TLR2 recognizes the cell wall components of Gram-positive bacteria including lipopeptides, peptidoglycan and lipoteichoic acids (LTAs) (9-11). By contrast, TLR4 senses lipopolysaccharide, a component of the outer membrane of Gram-negative bacteria (12-14). Thus, TLR-mediated signaling pathways are important for regulating antibacterial immune responses in neutrophils.

LTAs are found in the cell walls of many gram-positive bacteria, such as *Staphylococci*, *Streptococci*, *Bacilli* and *Listeria* (15). Different types of LTAs found in different bacterial species can be grouped according to their chemical structure (16). For example, type I LTAs are found in *Bacillus subtilis*, *Staphylococcus aureus* and *Listeria monocytogenes*, whereas type IV LTAs are found in *Streptococcus pneumoniae* (16). Exposure to *S. aureus*-derived LTA activates the TLR2 and NF-κB signaling pathways, increases production of ROS and induces the secretion of inflammatory molecules such as tumor necrosis factor-α (TNF-α), interleukin (IL)-1β and chemokine (C-X-C motif) ligand 8 (CXCL8, or IL-8) in human neutrophils (17-20).

Experimental studies on the molecular mechanisms and cell behaviors of primary human neutrophils are typically limited due to the short lifespan of human neutrophils (21,22). Therefore, a surrogate neutrophil-like cell line, such as the human promyelocytic leukemia cell line, HL-60, has been developed (23). HL-60 cells differentiate into a neutrophil-like phenotype *in vitro* (23). Differentiated HL-60 (dHL-60) cells serve as a good model for studying the phenotypes of human neutrophils, including chemotaxis, phagocytosis and the responses of TLR signaling pathways (24-27). Several protocols have been established for differentiating HL-60 cells into a neutrophil-like state using dimethyl sulfoxide (DMSO), N,N-dimethylformamide and all-trans retinoic acid (23,28,29). Reports have shown that different reagents induce the differentiation of HL-60 cells via different mechanisms (30,31), and that the characteristics of HL-60 cells differentiated by different methods are not completely identical to those of primary human neutrophils.

Although LTA-induced inflammatory responses have been studied in human neutrophils, comprehensive transcriptional regulation in LTA-treated neutrophil-like cells is not currently well understood. Specifically, there is a lack of relevant studies comparing LTA treatment at different time points and concentrations. Since DMSO-differentiated HL-60 cells can respond to TLR2 and TLR4 ligands (26), DMSO-induced neutrophil-like cells served as the experimental model in the present study. The present study investigated the transcriptional profiles of LTA-treated dHL-60 and LTA-treated undifferentiated HL-60 (uHL-60) cells, and further evaluated whether dHL-60 cells could be an alternative cell model for TLR studies in human neutrophils.

Materials and methods

Cell culture and differentiation. HL-60 cells were obtained from the Bioresource Collection and Research Center. The HL-60 cells were maintained in RPMI 1640 medium with L-glutamine (GeneDireX, Inc.) supplemented with 20% fetal bovine serum (Gibco; Thermo Fisher Scientific, Inc.) and antibiotics, including 100 U/ml penicillin, 100 μg/ml streptomycin and 0.25 μg/ml amphotericin B, at 37˚C in a humidified atmosphere with 5% CO_2. The cell density was maintained between $1x10^5$ and $1x10^6$ cells/ml. To differentiate the HL-60 cells into a neutrophil-like phenotype, the cells were cultured at a density of $1x10^6$ cells/ml in RPMI 1640 medium containing L-glutamine supplemented with 10% fetal bovine serum, 10 mM HEPES (Gibco; Thermo Fisher Scientific, Inc.), the aforementioned antibiotics and 1.25% DMSO for 6 days.

Evaluating NET formation, NETosis and ROS production in dHL-60 cells. To observe the induction of NETs in dHL-60 cells, dHL-60 cells were collected 6 days after DMSO stimulation. Extracellular DNA of NET were then visualized using SYTOX Green staining. Briefly, dHL-60 cells were seeded into 24-well plates ($2x10^5$ cells per well) in serum-free RPMI 1640 medium containing 1% bovine serum albumin and 1 mM calcium chloride, then treated with vehicle (DMSO) or 20 nM phorbol myristate acetate (PMA; MedChemExpress) at 37˚C. After 4 h, dHL-60 cells were stained with 5 μM SYTOX Green (Invitrogen; Thermo Fisher Scientific, Inc.) for 10 min in the dark at room temperature. Images were then obtained using a Nikon Eclipse TE2000-S inverted fluorescence microscope equipped with x10 magnification objectives. The experiment was repeated 3 times.

NET formation in dHL-60 cells was evaluated using a NETosis Assay Kit (Cayman Chemical Company). Briefly, $2x10^5$ dHL-60 cells were treated with either vehicle or PMA and then incubated at 37˚C for 4 h to induce NET formation, according to the manufacturer's instructions. After 4 h, the culture supernatant was collected and NET-associated neutrophil elastase activity was detected at 405 nm. The experiment was repeated 3 times.

ROS production in dHL-60 cells was detected by staining with a DCFDA/H2DCFDA-Cellular ROS Assay Kit (Abcam). After a 4-h stimulation with vehicle, 2 or 20 nM PMA, the dHL-60 cells were stained with 10 μM DCFDA for 30 min at 37˚C and then analyzed on a BD Accuri C6 Flow Cytometer (BD Biosciences), and the data were analyzed using FCSalyzer ver. 0.9.22-alpha (https://sourceforge.net/projects/fcsalyzer/). The experiment was repeated 2 times.

RNA sequencing. For RNA sequencing, $2x10^6$ uHL-60 cells were treated with 1 μg/ml *S. aureus* LTA (cat.no. L2515; Sigma-Aldrich; Merck KGaA) or vehicle (ddH2O) for 4 and 24 h (n=1), and $2x10^6$ dHL-60 cells were treated with 1 μg/ml or 10 μg/ml *S. aureus* LTA or vehicle (ddH2O) for 4 and 24 h (n=2) in 37˚C incubator with 5% CO_2. Total RNA from $2x10^6$ uHL-60 and dHL-60 cells was extracted using a Total RNA Purification Kit (Norgen Biotek Corp.). The purified RNA was used for the preparation of the sequencing library by TruSeq Stranded mRNA Library Prep Kit (Illumina, Inc.) following the manufacturer's recommendations. After the generation of double-strand cDNA and adenylation on 3' ends of DNA fragments, the adaptors were ligated and purified with AMPure XP system (Beckman Coulter, Inc.). The quality of the libraries was assessed on the Agilent Bioanalyzer 2100 system and a Real-Time PCR system. RNA sequencing was performed using the Illumina NovaSeq 6000 platform with 150 bp paired end read lengths and 20 million clean reads per sample by a commercial vendor (Genomics BioSci & Tech Co. Ltd.). The bases with low quality and sequences from adapters in raw data were removed using program fastp (version 0.20.0; https://github.com/OpenGene/fastp). The filtered reads were aligned to the reference genomes using HISAT2 (version 2.1.0; https://daehwankimlab.github.io/hisat2/). The software FeatureCounts (v2.0.1; https://subread.sourceforge.net) in Subread package was applied for the quantification of the gene abundance. For identification of differentially expressed genes (DEGs), DESeq2 (version 1.28.0; https://bioconductor.org/packages/release/bioc/html/DESeq2.html) and EdgeR (version 3.36.0; https://bioconductor.org/packages/release/bioc/html/edgeR.html) were used to analyze samples with and without biological replicates respectively. The criteria for DEGs were set at fold change ≥2.0 and $P<0.05$ in the dHL-60 cell group. Compared with the dHL-60 cells, the gene expression of uHL-60 was less affected by LTA treatment. Therefore, the criterion of DEGs for the uHL-60 cells was set at $P<0.05$, owing to the small number of DEGs. Raw and processed RNA sequencing data were uploaded to the Gene Expression Omnibus (GEO) database (https://www.ncbi.nlm.nih.gov/geo/query/acc.cgi?acc=GSE239859).

Bioinformatic analysis. The processed RNA sequencing data deposited as GSE239859 in GEO database was further analyzed through the following methods. Principal Component Analysis (PCA), heatmaps and bubble plots were constructed using the online web tool, Srplot (http://www.bioinformatics.com.cn/srplot), and Venn diagrams were compiled using the website http://bioinformatics.psb.ugent.be/webtools/Venn/. To perform Gene Ontology (GO) analysis (biological processes) and Kyoto Encyclopedia of Genes and Genomes (KEGG) pathways, the DEGs were analyzed using the Database for Annotation, Visualization, and Integrated Discovery (DAVID; v6.8; https://david.ncifcrf.gov/) (32). The identified DEGs of uHL-60 and dHL-60 were further processed as input data for the DAVID analyses. A significant difference was indicated by a $P<0.001$. The predicted gene-targeted microRNAs (miRNAs) were analyzed using the miRNet 2.0 website (https://www.mirnet.ca) (33). The interaction network was constructed using Cytoscape software 3.9.1 (https://cytoscape.org). Gene Set Enrichment Analysis (GSEA) was performed using the WeB-based GEne SeT Analysis Toolkit (http://www.webgestalt.org) (34). The gene set for the KEGG pathway analysis was obtained from the Molecular Signatures Database [curated gene sets, canonical pathways, KEGG analysis for human gene symbols; v2022.1; https://www.gsea-msigdb.org/gsea/index.jsp] (35), while a false discovery rate of <0.05 was set as the significance level. For GSEA analysis, all genes identified by RNA sequencing were as input data.

Reverse transcription-quantitative PCR (RT-qPCR). Total RNA of dHL-60 was extracted using a Total RNA Purification Kit (Norgen Biotek Corp.) and then reverse-transcribed to cDNA using an iScript™ cDNA Synthesis Kit (Bio-Rad Laboratories, Inc.) according to the manufacturer's instructions. All qPCR experiments were run on a QuantStudio 5 Real-Time PCR system (Applied Biosystems; Thermo Fisher Scientific, Inc.) using the SYBR Green I-based TB Green Premix Ex Taq II (Takara Bio, Inc.) and the program, 95˚C for 30 sec, 40 cycles of 95˚C for 3 sec, and 60˚C for 30 sec. The relative mRNA expression was normalized to the expression of the internal control, b-actin, using by $2^{-\Delta\Delta Cq}$ method (36). The nucleotide sequences for the primers used are listed in Table I.

Statistical analysis. Bar plots and statistical analyses were performed using GraphPad Prism 8.4.3 software (Dotmatics). A two-tailed unpaired t-test was used to analyze the differences between two groups. One-way ANOVA and Tukey's multiple-comparison test were used to compare three groups. $P<0.05$ was considered to indicate a statistically significant difference.

Table I. Primer sequences used in reverse transcription-quantitative polymerase chain reaction.

Primer name	Sequence (5'-3')
CCL2 forward	TCTGTGCCTGCTGCTCATAG
CCL2 reverse	TGGAATCCTGAACCCACTTC
CCL5 forward	CGTGCCCACATCAAGGAGTAT
CCL5 reverse	CGGTTCTTTCGGGTGACAAA
CXCL8 forward	TGTGTGTAAACATGACTTCCAAGCT
CXCL8 reverse	GCAAAACTGCACCTTCACACAG
IL-1β forward	TGAAAGATGATAAGCCCACTCTACA
IL-1β reverse	AGACTCAAATTCCAGCTTGTTATTG
TNF forward	CCCAGGCAGTCAGATCATCTTC
TNF reverse	GCTTGAGGGTTTGCTACAACATG
β-actin forward	TTAGTTGCGTTACACCCTTTCTTG
β-actin reverse	TCACCTTCACCGTTCCAGTTT

CCL, C-C motif chemokine ligand; CXCL8, C-X-C motif ligand 8; IL-1β, interleukin-1β; TNF, tumor necrosis factor.

Results

Evaluation of the neutrophil-like phenotypes of dHL-60 and the transcriptomes of differentiated and undifferentiated HL-60 cells. A flowchart of the present study is presented in Fig. 1A. To obtain neutrophil-like phenotypes, uHL-60 cells were differentiated by DMSO treatment. The neutrophil-like phenotype of dHL-60 cells was then further evaluated. PMA is a known inducer of NET formation and ROS production (37,38). Fluorescence microscopy revealed the formation of NETs in PMA-stimulated dHL-60 cells (Fig. 1B). The NETosis assay also demonstrated that PMA stimulation significantly increased NET-associated elastase activity (Fig. 1C). In addition, ROS production was increased following PMA stimulation (Fig. 1D). These results indicated that DMSO-differentiated HL-60 cells had neutrophil-like phenotypes.

The doses of 0.1-10 μg/ml *S. aureus* LTA are used in several published studies (18,20), and treatment with LTA >1 μg/ml induces relatively significant immune responses in immune cells. However, the present pretest experiments showed that treatments with 1 or 10 μg/ml *S. aureus* did not induce the expression of inflammatory molecules in uHL-60 as in human primary neutrophils (data not shown). Therefore, the current study focused on LTA-treated dHL-60, while udHL-60 was tested only at a single dose of LTA using a single sample. For RNA sequencing analysis, uHL-60 cells were treated with 1 μg/ml *S. aureus* LTA or vehicle (ddH_2O) for 4 and 24 h (n=1), and dHL-60 cells were treated with 1 μg/ml or 10 μg/ml *S. aureus* LTA or vehicle (ddH_2O) for 4 and 24 h (n=2). Subsequently, the gene expression profiles of the harvested cells were analyzed by RNA sequencing, and PCA was performed to examine the distribution of DEGs in each group. Fig. 2A and B show the differences in gene expression profiles between the uHL-60 and dHL-60 cells. The PCA plot demonstrated a clear separation between the uHL-60 and dHL-60 cells, and LTA-treated dHL-60 and vehicle-treated dHL-60 were also distributed in two clusters. By contrast, there was no clear separation of LTA-treated uHL-60 and vehicle-treated uHL-60 cells at either time point. A heatmap plot revealed similar clusters among the uHL-60 and dHL-60 cell samples (Fig. S1).

The Venn diagram demonstrated that various shared DEGs were identified in the 'LTA1 vs. Vehicle' and 'LTA10 vs. Vehicle' groups for the dHL-60 cells at both time points

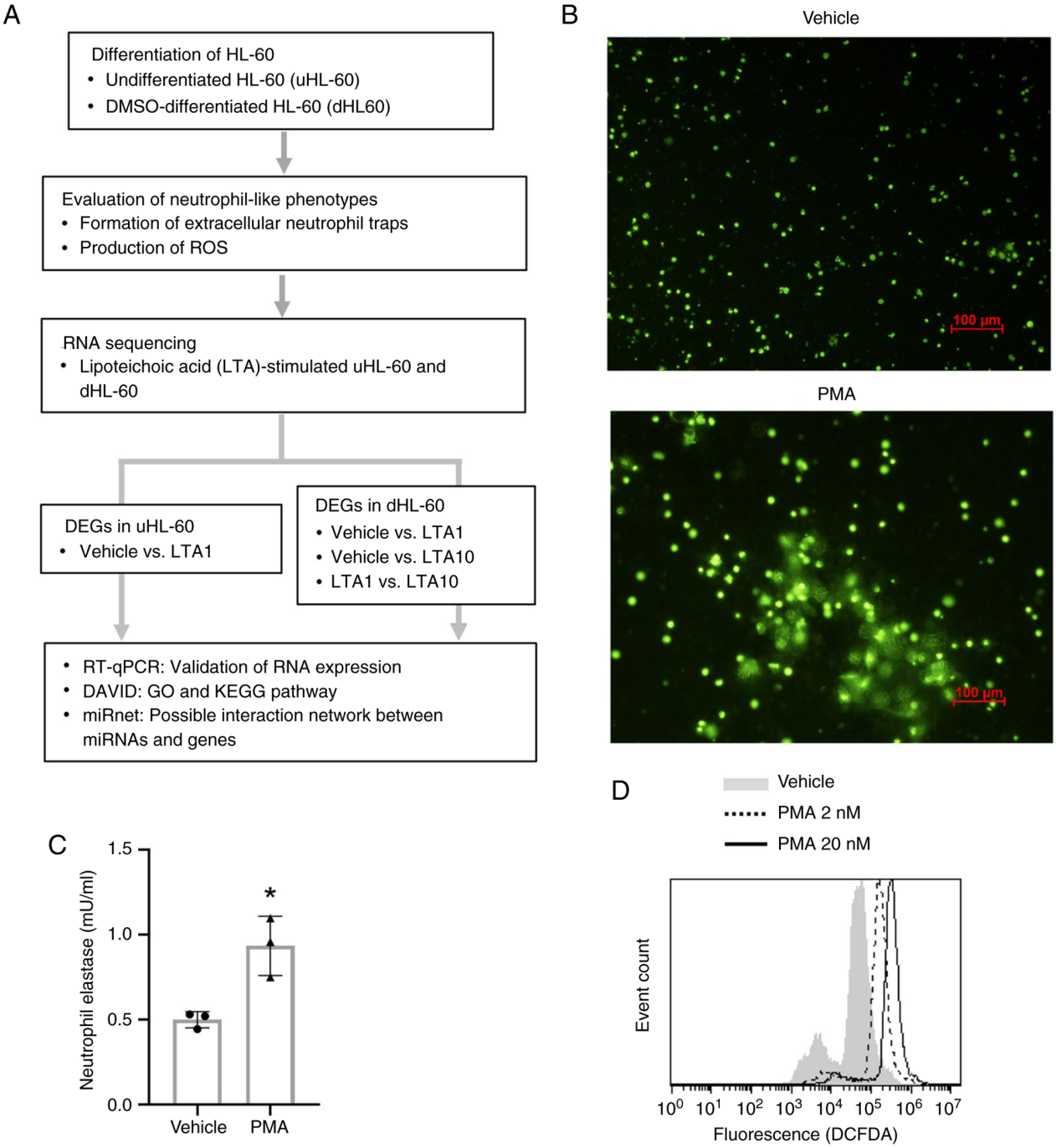

Figure 1. Overall study design and the neutrophil-like phenotypes of dHL-60 cells. (A) Flowchart of the present study. Differentiation of HL-60 cells was induced by DMSO treatment, and then the neutrophil-like phenotypes of dHL-60 cells were confirmed. To investigate the gene expression profiles of LTA-treated uHL-60 and dHL-60 cells, uHL-60 cells were treated with vehicle (ddH_2O) or 1 μg/ml *S. aureus* LTA for 4 and 24 h (n=1), and dHL-60 cells were treated with vehicle (ddH_2O), 1 μg or 10 μg of *S. aureus* LTA (n=2). The cell samples were then analyzed via RNA sequencing. DEGs in each group were merged using Venn diagrams, and then the expression levels of genes were further validated by RT-qPCR. The GO and KEGG pathway analysis was performed using DAVID, and the predicted miRNA-gene interaction was analyzed by miRnet. (B) Formation of NETs were detected by fluorescent microscopy. Following treatment with 20 nM PMA or vehicle (DMSO) for 4 h, the samples were stained with SYTOX Green (magnification, x10; scale bar, 100 μm). Because SYTOX Green stain does not penetrate living dHL-60, untreated live dHL-60 cells showed little or no fluorescence. By contrast, extracellular DNA of NET induced by PMA were stained with SYTOX Green fluorescence. (C) The activity of neutrophil elastase was measured following treatment with 20 nM PMA or vehicle (DMSO) for 4 h. Data presented as the mean ± standard deviation. *P<0.05, determined using an unpaired t-test. (D) Flow cytometry of H2DCFDA staining for ROS in dHL-60 cells following treatment with 2 or 20 nM PMA or vehicle (DMSO) for 4 h. DAVID, Database for Annotation, Visualization; DEGs, differentially expressed genes; DMSO, dimethyl sulfoxide; GO, Gene Ontology; dHL-60, differentiated HL-60; LTA, lipoteichoic acid; KEGG, Kyoto Encyclopedia of Genes and Genomes; LTA1, cells treated with 1 μg/ml LTA; LTA10, cells treated with 10 μg/ml LTA; miRNAs, microRNAs; PMA, phorbol myristate acetate; ROS, reactive oxygen species; RT-qPCR, reverse transcription-quantitative PCR; uHL-60, undifferentiated HL-60.

(Fig. 2C and D). However, only 1 shared DEG [C-C motif chemokine ligand 1 (*CCL1*)] and 2 shared DEGs (hemoglobin subunit β and spermatogenesis and oogenesis specific basic helix-loop-helix 2 genes) were identified in the three groups comparison at 4 and 24 h, respectively. The results showed that the transcript levels of uHL-60 cells were

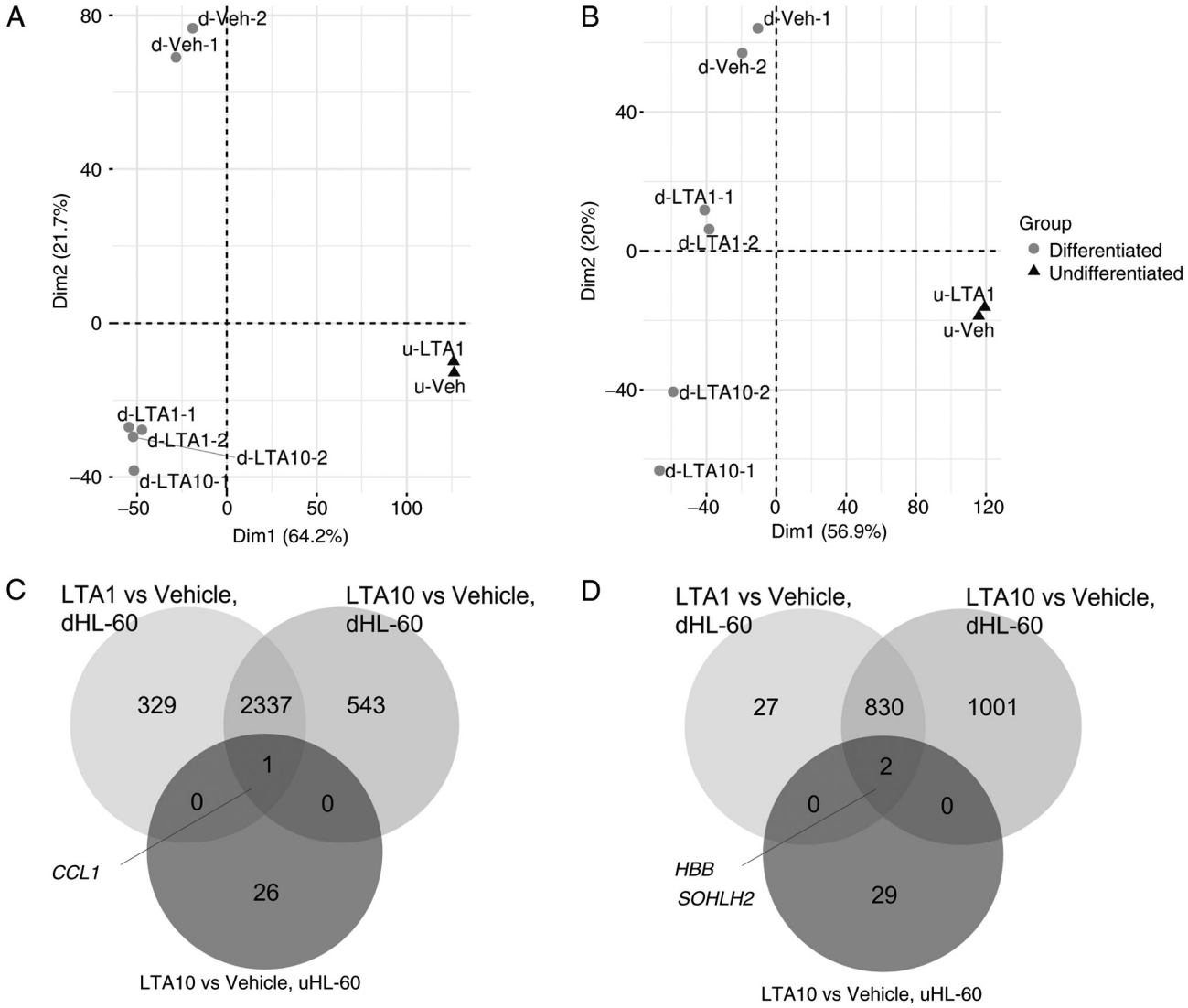

Figure 2. Principal component analysis of uHL-60 and dHL-60 cells treated with LTA and vehicle (DMSO) for (A) 4 and (B) 24 h. Differentially expressed genes from 'LTA1 vs. Vehicle' in uHL-60 cells, 'LTA1 vs. Vehicle' in dHL-60 cells and 'LTA10 vs. Vehicle' in dHL-60 cells were merged in a the Venn diagram to identify the shared genes among these three groups following (C) 4 and (D) 24 h of LTA treatment. CCL1, C-C motif chemokine ligand 1; DMSO, dimethyl sulfoxide; dHL-60, differentiated HL-60; HBB, hemoglobin subunit b; LTA, lipoteichoic acid; LTA1, cells treated with 1 μg/ml LTA; LTA10, cells treated with 10 μg/ml LTA; SOHLH2, spermatogenesis and oogenesis specific basic helix-loop-helix 2; uHL-60, undifferentiated HL-60.

completely different from those of dHL-60 cells after LTA treatment. The results suggested that uHL60 and dHL60 indeed had different characteristics, and their responses to LTA treatment were almost completely different. Therefore, the enriched pathways in uHL-60 and dHL-60 cells were investigated separately.

LTA-affected pathways in uHL-60 cells. The functions of the identified DEGs in uHL-60 cells after 4 and 24 h of LTA treatment were annotated by GO analysis using DAVID. No significant pathways were enriched after 4 h of LTA treatment. The enriched pathways in uHL-60 cells after 24 h of LTA treatment are shown in Table II. Most of the identified pathways were associated with survival of motor neuron 1, telomeric (*SMN1*) and survival of motor neuron 2, centromeric (*SMN2*) genes. The results therefore suggested that treatment with 1 μg/ml LTA affected only a small proportion of genes in uHL-60 cells.

LTA-affected pathways in dHL-60 cells. A large number of common DEGs were identified in the 1 μg/ml LTA (LTA1) and 10 μg/ml LTA (LTA10) treated dHL-60 cells at both time points (Fig. 2C and D). Compared with the vehicle group, increased expression levels of known LTA-induced inflammatory molecules were observed in the LTA1 and LTA10 groups, according to the RNA sequencing data (Fig. 3A and B). To further confirm the observed expression profiles, the mRNA expression levels of CCL2, CCL5, CXCL8, IL-1β and TNF were quantified using RT-qPCR. In general, the expression patterns of these molecules in the RT-qPCR analysis were similar to those observed in the RNA sequencing analysis (Fig. 3C-G).

To further investigate the enriched pathways in LTA-treated dHL-60 cells, GO (biological processes) and KEGG pathway analyses were performed using DAVID, according to the common upregulated 1,234 and 718 DEGs in the 4 and 24 h LTA-treated groups, respectively

Table II. GO enriched pathways in undifferentiated HL-60 cells following 24 h of lipoteichoic acid treatment.

GO term	Count	P-value	Genes
GO:0006353, DNA-templated transcription, termination (BP)	2	0.0075	SMN2, SMN1
GO:0000245, spliceosomal complex assembly (BP)	2	0.0161	SMN2, SMN1
GO:0000387, spliceosomal snRNP assembly (BP)	2	0.0173	SMN2, SMN1
GO:0032797, SMN complex (CC)	2	0.0092	SMN2, SMN1
GO:0097504, Gemini of coiled bodies (CC)	2	0.0111	SMN2, SMN1
GO:0031083, BLOC-1 complex (CC)	2	0.0120	BLOC1S5, BLOC1S5-TXNDC5
GO:0034719, SMN-Sm protein complex (CC)	2	0.0166	SMN2, SMN1

BP, Biological Processes; BLOC1S5, biogenesis of lysosomal organelles complex 1 subunit 5; CC, Cellular Component; GO, gene ontology; SMN1, survival of motor neuron 1, telomeric; SMN2, survival of motor neuron 2, centromeric; TXNDC5, thioredoxin domain containing 5.

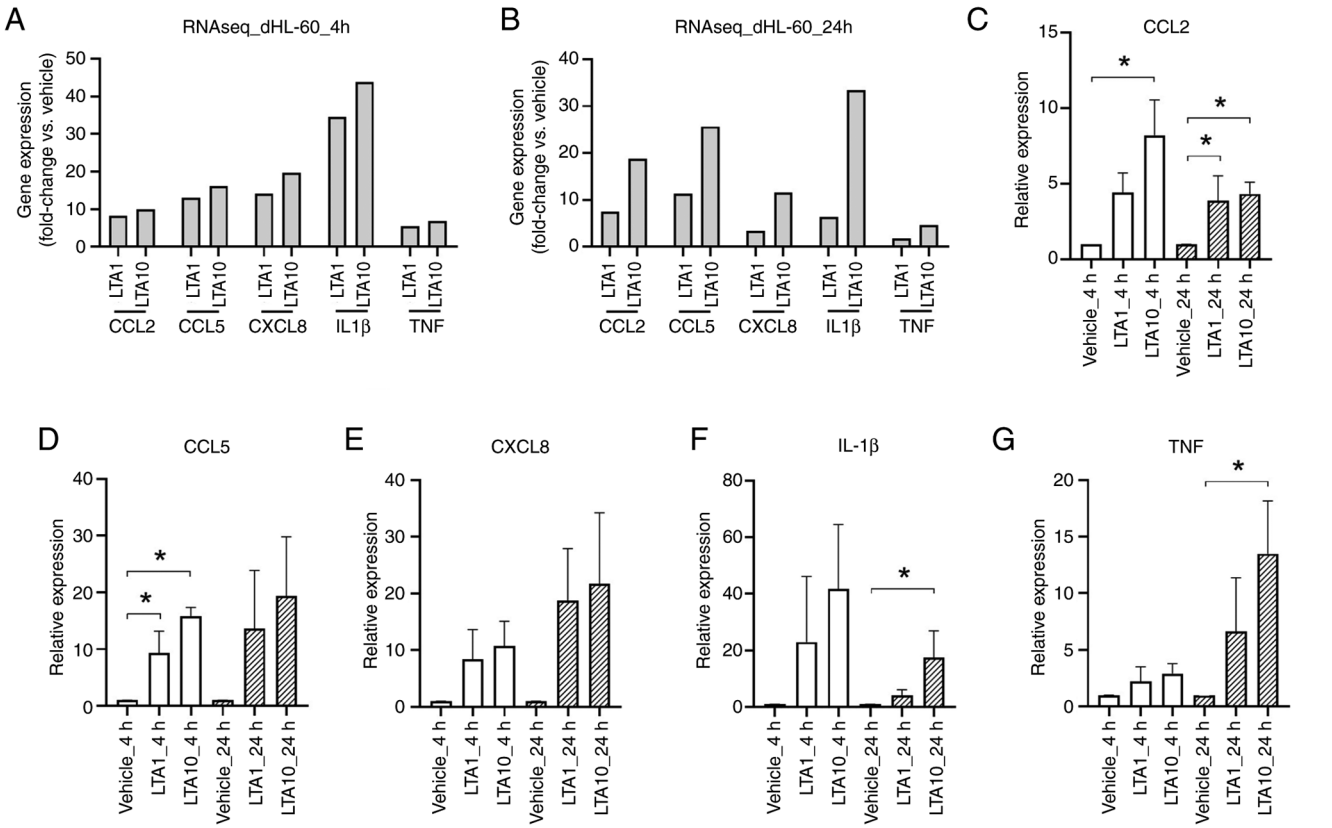

Figure 3. Expression of LTA-induced inflammatory molecules in dHL-60 cells. After RNAseq analysis, the fold change (LTA-treated group/vehicle group) of each gene was determined following (A) 4 and (B) 24 h of LTA treatment. The relative expression levels of (C) CCL2, (D) CCL5, (E) CXCL8, (F) IL-1β and (G) TNF were determined using reverse transcription-quantitative polymerase chain reaction. Data are presented as the mean ± standard deviation. *P<0.05 vs. Vehicle, determined using one-way ANOVA and Tukey's multiple-comparison test. CCL, C-C motif chemokine ligand; CXCL8, C-X-C motif ligand 8; dHL-60, differentiated HL-60; IL-1β, interleukin-1β; LTA1, cells treated with 1 μg/ml LTA; LTA10, cells treated with 10 μg/ml LTA; TNF, tumor necrosis factor; RNAseq, RNA sequencing.

(Fig. 4A and B). Fig. 4C-F show the identified top 10 significantly enriched biological processes and KEGG pathways. The top 20 biological processes, KEGG pathways and detailed gene lists are presented in Tables SI-SIV. Numerous identical biological processes were observed including 'inflammatory response', 'cellular response to lipopolysaccharide', 'immune response', 'cellular response to tumor necrosis factor', 'signal transduction', 'apoptotic process', 'chemokine-mediated signaling pathway', 'positive regulation of inflammatory response', 'neutrophil chemotaxis', 'positive regulation of cell migration', 'chemotaxis' and 'positive regulation of ERK1 and ERK2 cascade' in the 4 or 24 h LTA-treated groups. Furthermore, identical KEGG pathways including 'Cytokine-cytokine receptor interaction', 'TNF signaling pathway', 'Viral protein interaction with cytokine and cytokine receptor', 'Lipid and atherosclerosis',

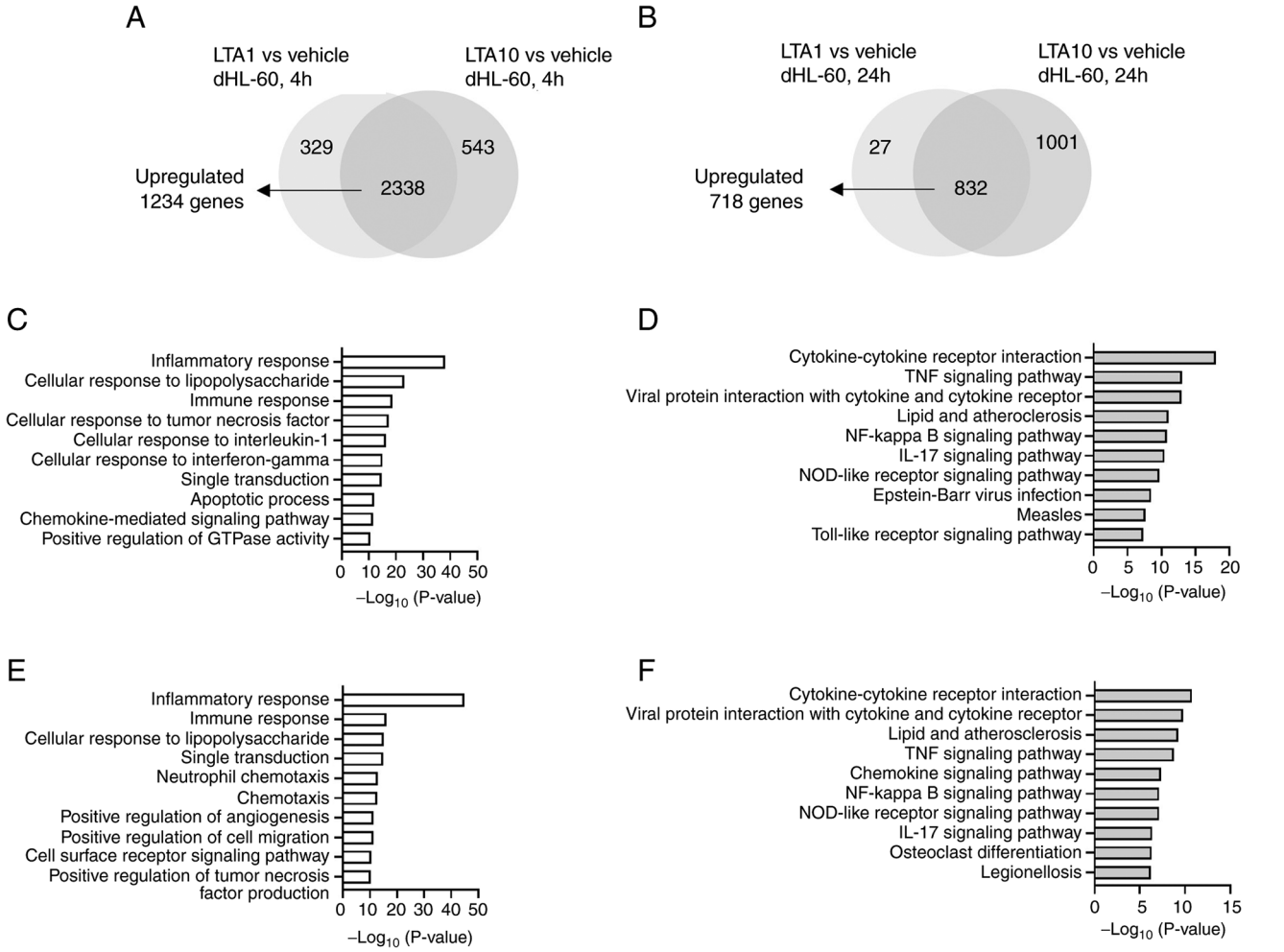

Figure 4. GO and KEGG pathway analyses of the shared upregulated DEGs in dHL-60 cells following 4 and 2 h of LTA treatment. Venn diagrams showing the shared upregulated DEGs between 'LTA1 vs. vehicle' and 'LTA10 vs. vehicle' in dHL-60 cells after (A) 4 and (B) 24 h of LTA treatment. Top 10 shared enriched GO biological processes after (C) 4 and (D) 24 h of LTA treatment are presented in a bar chart. Top 10 shared enriched KEGG pathways after (E) 4 and (F) 24 h of LTA treatment are presented in a bar chart. DEGs, differentially expressed genes; dHL-60, differentiated HL-60; GO, Gene Ontology; LTA, lipoteichoic acid; KEGG, Kyoto Encyclopedia of Genes and Genomes; LTA1, cells treated with 1 μg/ml LTA; LTA10, cells treated with 10 μg/ml LTA.

'NF-kappa B signaling pathway', 'IL-17 signaling pathway', 'NOD-like receptor signaling pathway', 'Toll-like receptor signaling pathway', 'Chemokine signaling pathway' and 'Rheumatoid arthritis' were observed in the top 20 enriched KEGG pathways. Therefore, the results demonstrated that the enriched pathways following 4 and 24 h LTA treatment of dHL-60 cells were similar.

Our previous study demonstrated that the expression levels of four miRNAs, including hsa-miR-34a-5p, hsa-miR-34c-5p, hsa-miR-708-5p and hsa-miR-1271-5p, are affected by LTA treatment in human primary neutrophils (39). Although the present study aimed to determine whether the same miRNA is regulated in LTA-treated dHL-60 cells, microRNA sequencing was not performed in this study. Therefore, the miRNAs that were predicted to interact with the commonly upregulated DEGs in the 4 or 24 h LTA-treated groups were analyzed using the miRnet website. The above four miRNAs were also included in the list of miRNAs predicted to interact with the upregulated DEGs. These results implied that similar miRNA-gene interactions can be found in both human primary neutrophils and dHL-60 cells treated with LTA. A possible interaction network between the shared upregulated DEGs in LTA-treated dHL-60 and the aforementioned four miRNAs is shown in Fig. 5.

Effect of low and high dose LTA treatment in dHL-60 cells. The impact of high and low concentrations of LTA on dHL-60 cells was further investigated by comparing the enriched pathways between the two groups. A volcano plot presenting the DEGs between the LTA1 and LTA10-treated dHL-60 cells is shown in Fig. S2. The results revealed that less DEGs were found in the samples treated for 4 h compared with the samples treated for 24 h. GSEA was performed to further investigate the enriched pathways in both groups. The 'Complement and coagulation cascades' was the only pathway that reached statistical significance (false discovery rate <0.05) in the LTA1 cells treated for 4 h (Fig. 6A). By contrast, multiple significantly enriched KEGG pathways were observed in the LTA10 cells treated for 24 h (Fig. 6B-L). Several immune response-related pathways were enriched, including 'Cytokine-cytokine receptors interaction,' 'Chemokine signaling pathways,' 'Toll-like receptor signaling pathway,' 'NOD like receptor signaling pathway' and 'Cytosolic DNA sensing pathway.' These enriched pathways were associated with innate immune responses.

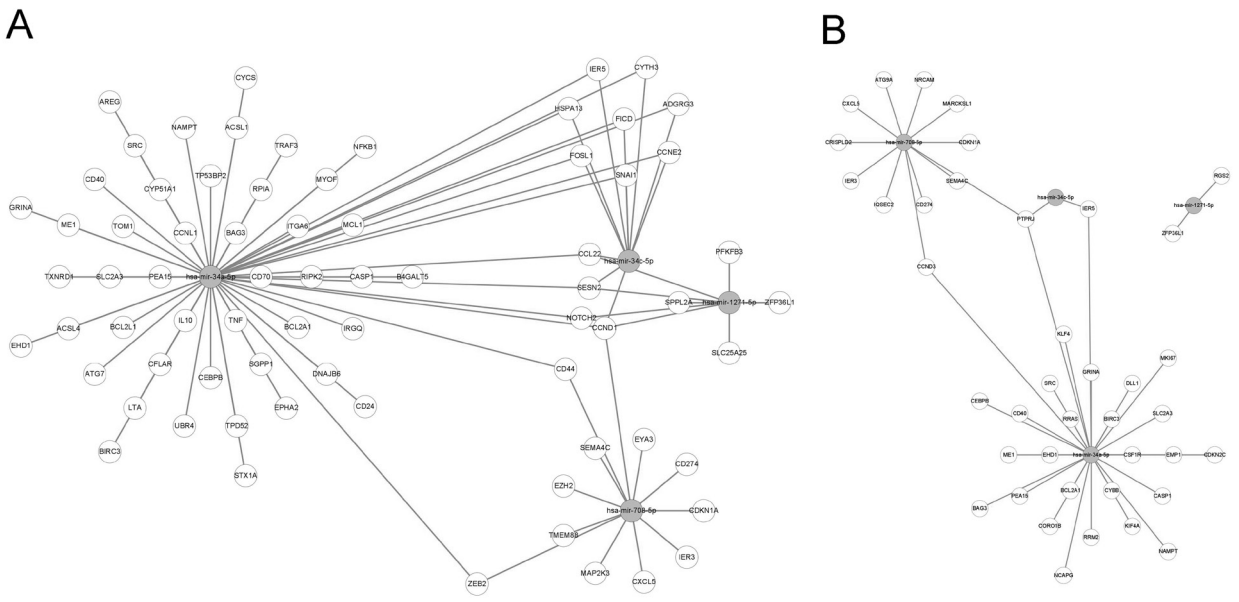

Figure 5. Interactions of genes and predicted target miRNAs. The shared upregulated genes in the 4 and 24 h treatment groups were selected for analysis, and the potential target miRNAs were predicted using the miRnet website. The resulting predicted interactions between selected genes and miRNAs, including hsa-miR-34a-5p, hsa-miR-34c-5p hsa-miR-708-5p and hsa-miR-1271-5p, following (A) 4 and (B) 24 h of lipoteichoic acid treatment are shown. The circles filled with white color represent genes and the circles filled with gray color represent miRNAs. miR/miRNA, microRNA.

Discussion

In the present study, uHL-60 cells were only treated with a single concentration of LTA (1 μg/ml) for 4 and 24 h. RNA sequencing revealed that only a few genes were affected by this LTA treatment. No significantly enriched pathways were found following GO and KEGG analyses in the 4-h LTA treatment group. By contrast, some biological processes reached statistical significance in the 24-h LTA treatment group. In total, 4 genes, including the protein-coding genes *SMN1*, *SMN2* and biogenesis of lysosomal organelles complex 1 subunit 5 (*BLOC1S5*), and the non-protein-coding gene BLOC1S5-TXNDC5 readthrough (NMD candidate) (*BLOC1S5-TXNDC5*), are involved in these biological processes. SMN1 and SMN2 play important roles in small nuclear ribonucleoproteins (40), and the functions of BLOC1S5 and BLOC1S5-TXNDC5 are associated with the BLOC-1 complex (41). However, the mechanism by which SMN1, SMN2 and BLOC-1 complexes are regulated by LTA treatment remains unknown. Overall, uHL-60 cells treated with LTA showed a transcriptional profile completely different from that of LTA-treated dHL-60.

In previous studies, the *S. aureus* LTA-induced immune responses in human neutrophils have been investigated over <6 h or following 16 and 24 h of treatment at concentrations of LTA ranging 1-10 μg/ml (17,18,39). A DMSO-differentiated HL-60 cell model has also been used previously to investigate the functions of neutrophils, including cell polarization, ROS production, chemotaxis, NETosis and phagocytosis, which the present study aimed to further confirm (42). The present study investigated the effects of *S. aureus* LTA on DMSO-treated dHL-60 cells. The experimental conditions used in the present study, including the LTA concentrations and time points, were set according to previous reports.

LTA stimulation activates TLR2 signaling and the pro-inflammatory cytokine response, including TNF-α, IL-1β and CXCL8, in human neutrophils (17-20). In addition, CXCL8 recruits more neutrophils and immune cells (43), and prolongs the lifespan of neutrophils (17). In addition, *S. aureus* infection can be recognized by TLR, nucleotide binding oligomerization domain (NOD) and C-type lectin (CLR) receptors (44). Th17 signaling is also activated following LTA stimulation (45). In the present study, the RNA sequencing results demonstrated that hundreds of identical DEGs were found in samples treated with 1 and 10 μg/ml LTA for 4 and 24 h. According to the GO and KEGG pathway analyses of DEGs with upregulated expression, biological processes and KEGG pathways, such as 'immune response', 'inflammatory response', 'Cytokine-cytokine receptor interaction', 'TNF signaling pathway', 'Toll-like receptor pathway', 'IL-17 signaling pathway', 'NOD-like receptor signaling pathway' and 'NF-kappa B signaling pathway' were significantly enriched in LTA-treated dHL-60 cells at both time points. Interferon γ (IFN-γ) is a cytokine that promotes Th1 cell development (46), and the presence of IFN-γ could enhance CCL2 production in LTA-treated neutrophils (47). In the present study, significantly high CCL2 expression was observed by RNA sequencing and RT-qPCR analysis, which may suggest that the enriched IFN-γ signaling pathways also enhanced CCL2 and chemokine signaling pathways in LTA-treated dHL-60 cells. In summary, the known LTA-induced signaling pathways in human neutrophils were also observed in 1 and 10 μg/ml LTA-treated dHL-60 cells following 4 and 24 h of treatment. This suggested that dHL-60 cells could serve as an *in vitro* model for investigating TLR2 signaling pathways in human neutrophils.

The effects of different LTA concentrations on dHL-60 cells were also determined in the present study. Due to the relatively small number of DEGs observed between the

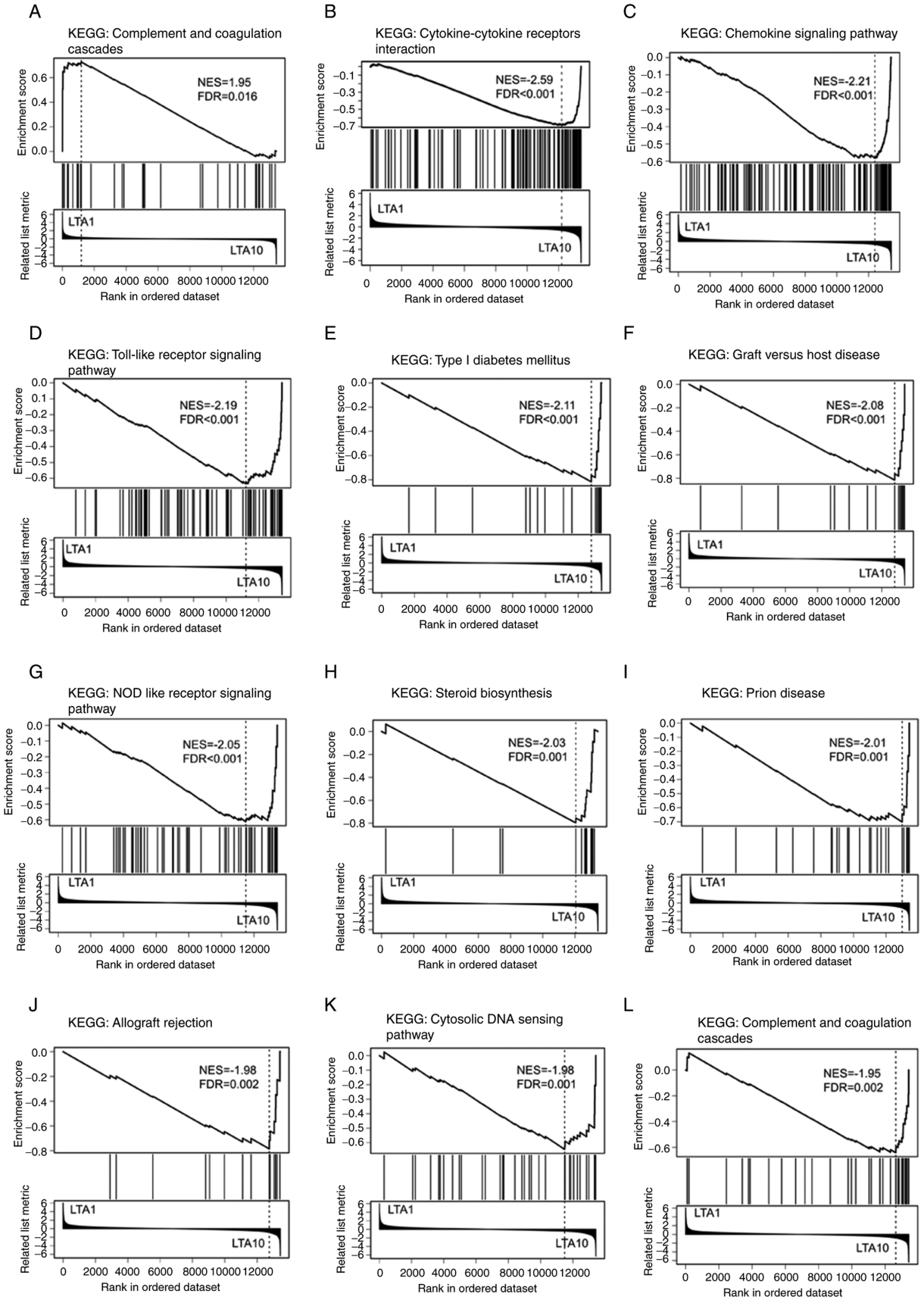

Figure 6. Analytical results of the Gene Set Enrichment Analysis of DEGs between the LTA1 and LTA10 samples. The KEGG pathway gene set was used to analyze the DEGs. Enrichment plots showing the significantly enriched KEGG terms (FDR<0.05), including (A) 'Complement and coagulation cascades' pathway enriched in LTA1, and (B) 'Cytokine-cytokine receptors interaction', (C) 'Chemokine signaling pathway', (D) 'Toll-like receptor signaling pathway', (E) 'Type I diabetes mellitus', (F) 'Graft vs. host disease', (G) 'NOD like receptor signaling pathway', (H) 'Steroid biosynthesis', (I) 'Prion disease', (J) 'Allograft rejection', (K) 'Cytosolic DNA sensing pathway' and (L) 'Complement and coagulation cascades' pathways enriched in LTA10. DEGs, differentially expressed genes; FDR, false discovery rate; LTA, lipoteichoic acid; KEGG, Kyoto Encyclopedia of Genes and Genomes; LTA1, cells treated with 1 μg/ml LTA; LTA10, cells treated with 10 μg/ml LTA; NES, normalized enrichment score.

1 and 10 μg/ml treated groups, GSEA analysis was performed instead of over-representation analysis. Only the 'Complement and coagulation cascades' was a significantly enriched KEGG pathway in the 1 μg/ml 4-h LTA-treated dHL-60 cells, while no KEGG pathways were significantly enriched in the 1 μg/ml 4-h LTA-treated uHL-60 cells. By contrast, several significantly enriched pathways were observed in the 10 μg/ml 24-h LTA-treated dHL-60 cells. These enriched pathways, including 'Cytokine-cytokine receptor interaction', 'Chemokine signaling pathway', 'Toll-like receptor signaling pathway', 'NOD-like receptor signaling pathway' and 'Cytosolic DNA sensing pathway' are associated with or are downstream of TLR signaling pathways (6). Furthermore, other identified pathways, such as 'Type I diabetes mellitus', 'Graft vs. host disease', 'Prion disease', 'Steroid biosynthesis' and 'Allograft rejection' are associated with innate immune responses (48-52). The 'Complement and coagulation cascade' was also enriched in both the 1 μg/ml 4-h LTA-treated dHL-60 cells and the 10 μg/ml 24-h LTA-treated dHL-60 cells. The complement and coagulation pathways are important for the host defense functions of neutrophils (53). However, this is related to the mechanism by which *S. aureus* evades phagocytosis (54). Altogether, it was discovered that all enriched pathways were associated with TLR signaling pathways in neutrophils, although there were some differences in gene expression between the high and low concentrations of LTA treatment for 4 and 24 h.

Bacterial infection alters the expression of inflammation-related miRNAs *in vivo* (55). For example, miR-142 is essential for the clearance of *S. aureus* infections at skin wound sites via neutrophil regulation (56). In addition, targeting miR-223 and miR-139-5p may serve as a therapeutic strategy to enhance the clearance of *S. aureus* infections in skin wounds (57,58). Our previous study identified several differentially expressed miRNAs using small RNA sequencing in LTA-stimulated primary human neutrophils (39). Although small RNA sequencing was not performed in the present study, predictive tools were used to determine whether dHL-60 cells have a regulatory network similar to that of human neutrophils. In total, hundreds of miRNAs were identified in the prediction results, which also included the same miRNAs as previously identified in primary human neutrophils (39). However, these interactions should be experimentally verified in future studies.

The present study had some limitations. For example, there is a gap between transcription, translation and post-translational processes. Therefore, the change in transcriptional levels may not necessarily be reflected in the protein levels. As such, the protein levels of LTA-treated dHL-60 cells need to be validated. Furthermore, the effect of LTA on primary human neutrophils under similar experimental conditions was not investigated. These issues require further investigation.

In summary, RNA sequencing of LTA-treated dHL-60 cells confirmed that the enriched pathways following treatment were associated with TLR signaling pathways at the two tested time points. A comparison of different LTA concentrations also revealed that TLR and TLR-related signaling pathways were enriched following treatment. This further suggested that DMSO-differentiated HL-60 cells may be a suitable alternative model for studying human neutrophils.

Acknowledgements

Not applicable.

Funding

This research was supported by grants from the Ministry of Science and Technology (MOST) of Taiwan (grant no. MOST 107-2320-B-037-011-MY3) and Kaohsiung Medical University Hospital (grant nos. KMUH107-7M36, KMUH109-9R82, KMUH110-0M75 and KMUH111-1M61).

Availability of data and materials

The data generated in the present study may be requested from the corresponding author.

Authors' contributions

KL and MY conceived and designed the study. KL, IY, YH and MY acquired, analyzed and interpreted the data. KL and MY drafted the manuscript. KL and MY confirm the authenticity of all the raw data. All the authors have read and approved the final version of the manuscript.

Ethics approval and consent to participate

Not applicable.

Patient consent for publication

Not applicable.

Competing interests

The authors declare that that they have no competing interests.

References

1. Sagiv JY, Michaeli J, Assi S, Mishalian I, Kisos H, Levy L, Damti P, Lumbroso D, Polyansky L, Sionov RV, *et al*: Phenotypic diversity and plasticity in circulating neutrophil subpopulations in cancer. Cell Rep 10: 562-573, 2015.
2. Mantovani A, Cassatella MA, Costantini C and Jaillon S: Neutrophils in the activation and regulation of innate and adaptive immunity. Nat Rev Immunol 11: 519-531, 2011.
3. Brubaker SW, Bonham KS, Zanoni I and Kagan JC: Innate immune pattern recognition: A cell biological perspective. Annu Rev Immunol 33: 257-290, 2015.
4. Mogensen TH: Pathogen recognition and inflammatory signaling in innate immune defenses. Clin Microbiol Rev 22: 240-273, Table of Contents, 2009.
5. Borregaard N: Neutrophils, from marrow to microbes. Immunity 33: 657-670, 2010.
6. Kawasaki T and Kawai T: Toll-like receptor signaling pathways. Front Immunol 5: 461, 2014.
7. Hayashi F, Means TK and Luster AD: Toll-like receptors stimulate human neutrophil function. Blood 102: 2660-2669, 2003.
8. Cook DN, Pisetsky DS and Schwartz DA: Toll-like receptors in the pathogenesis of human disease. Nat Immunol 5: 975-979, 2004.
9. Seo HS, Michalek SM and Nahm MH: Lipoteichoic acid is important in innate immune responses to gram-positive bacteria. Infect Immun 76: 206-213, 2008.
10. Schwandner R, Dziarski R, Wesche H, Rothe M and Kirschning CJ: Peptidoglycan- and lipoteichoic acid-induced cell activation is mediated by toll-like receptor 2. J Biol Chem 274: 17406-17409, 1999.

11. Oliveira-Nascimento L, Massari P and Wetzler LM: The role of TLR2 in infection and immunity. Front Immunol 3: 79, 2012.
12. Lu YC, Yeh WC and Ohashi PS: LPS/TLR4 signal transduction pathway. Cytokine 42: 145-151, 2008.
13. Park BS and Lee JO: Recognition of lipopolysaccharide pattern by TLR4 complexes. Exp Mol Med 45: e66, 2013.
14. Miller SI, Ernst RK and Bader MW: LPS, TLR4 and infectious disease diversity. Nat Rev Microbiol 3: 36-46, 2005.
15. Weidenmaier C and Peschel A: Teichoic acids and related cell-wall glycopolymers in gram-positive physiology and host interactions. Nat Rev Microbiol 6: 276-287, 2008.
16. Percy MG and Gründling A: Lipoteichoic acid synthesis and function in gram-positive bacteria. Annu Rev Microbiol 68: 81-100, 2014.
17. Lotz S, Aga E, Wilde I, van Zandbergen G, Hartung T, Solbach W and Laskay T: Highly purified lipoteichoic acid activates neutrophil granulocytes and delays their spontaneous apoptosis via CD14 and TLR2. J Leukoc Biol 75: 467-477, 2004.
18. Hattar K, Grandel U, Moeller A, Fink L, Iglhaut J, Hartung T, Morath S, Seeger W, Grimminger F and Sibelius U: Lipoteichoic acid (LTA) from Staphylococcus aureus stimulates human neutrophil cytokine release by a CD14-dependent, Toll-like-receptor-independent mechanism: Autocrine role of tumor necrosis factor-[alpha] in mediating LTA-induced interleukin-8 generation. Crit Care Med 34: 835-841, 2006.
19. van Kessel KP, Bestebroer J and van Strijp JA: Neutrophil-mediated phagocytosis of Staphylococcus aureus. Front Immunol 5: 467, 2014.
20. Schröder NW, Morath S, Alexander C, Hamann L, Hartung T, Zähringer U, Göbel UB, Weber JR and Schumann RR: Lipoteichoic acid (LTA) of Streptococcus pneumoniae and Staphylococcus aureus activates immune cells via Toll-like receptor (TLR)-2, lipopolysaccharide-binding protein (LBP), and CD14, whereas TLR-4 and MD-2 are not involved. J Biol Chem 278: 15587-15594, 2003.
21. Summers C, Rankin SM, Condliffe AM, Singh N, Peters AM and Chilvers ER: Neutrophil kinetics in health and disease. Trends Immunol 31: 318-324, 2010.
22. Kolaczkowska E and Kubes P: Neutrophil recruitment and function in health and inflammation. Nat Rev Immunol 13: 159-175, 2013.
23. Collins SJ, Ruscetti FW, Gallagher RE and Gallo RC: Terminal differentiation of human promyelocytic leukemia cells induced by dimethyl sulfoxide and other polar compounds. Proc Natl Acad Sci USA 75: 2458-2462, 1978.
24. Wang D, Sennari Y, Shen M, Morita K, Kanazawa T and Yoshida Y: ERK is involved in the differentiation and function of dimethyl sulfoxide-induced HL-60 neutrophil-like cells, which mimic inflammatory neutrophils. Int Immunopharmacol 84: 106510, 2020.
25. Poplutz MK, Wessels I, Rink L and Uciechowski P: Regulation of the interleukin-6 gene expression during monocytic differentiation of HL-60 cells by chromatin remodeling and methylation. Immunobiology 219: 619-626, 2014.
26. Shuto T, Furuta T, Cheung J, Gruenert DC, Ohira Y, Shimasaki S, Suico MA, Sato K and Kai H: Increased responsiveness to TLR2 and TLR4 ligands during dimethylsulfoxide-induced neutrophil-like differentiation of HL-60 myeloid leukemia cells. Leuk Res 31: 1721-1728, 2007.
27. Wen SH, Hong ZW, Chen CC, Chang HW and Fu HW: Helicobacter pylori neutrophil-activating protein directly interacts with and activates Toll-like receptor 2 to induce the secretion of interleukin-8 from neutrophils and ATRA-induced differentiated HL-60 cells. Int J Mol Sci 22: 11560, 2021.
28. Graziano RF, Ball ED and Fanger MW: The expression and modulation of human myeloid-specific antigens during differentiation of the HL-60 cell line. Blood 61: 1215-1221, 1983.
29. Atkinson JP and Jones EA: Biosynthesis of the human C3b/C4b receptor during differentiation of the HL-60 cell line. Identification and characterization of a precursor molecule. J Clin Invest 74: 1649-1657, 1984.
30. Manda-Handzlik A, Bystrzycka W, Wachowska M, Sieczkowska S, Stelmaszczyk-Emmel A, Demkow U and Ciepiela O: The influence of agents differentiating HL-60 cells toward granulocyte-like cells on their ability to release neutrophil extracellular traps. Immunol Cell Biol 96: 413-425, 2018.
31. Babatunde KA, Wang X, Hopke A, Lannes N, Mantel PY and Irimia D: Chemotaxis and swarming in differentiated HL-60 neutrophil-like cells. Sci Rep 11: 778, 2021.
32. Huang da W, Sherman BT and Lempicki RA: Systematic and integrative analysis of large gene lists using DAVID bioinformatics resources. Nat Protoc 4: 44-57, 2009.
33. Chang L, Zhou G, Soufan O and Xia J: miRNet 2.0: Network-based visual analytics for miRNA functional analysis and systems biology. Nucleic Acids Res 48 (W1): W244-W251, 2020.
34. Liao Y, Wang J, Jaehnig EJ, Shi Z and Zhang B: WebGestalt 2019: Gene set analysis toolkit with revamped UIs and APIs. Nucleic Acids Res 47 (W1): W199-W205, 2019.
35. Subramanian A, Tamayo P, Mootha VK, Mukherjee S, Ebert BL, Gillette MA, Paulovich A, Pomeroy SL, Golub TR, Lander ES and Mesirov JP: Gene set enrichment analysis: A knowledge-based approach for interpreting genome-wide expression profiles. Proc Natl Acad Sci USA 102: 15545-15550, 2005.
36. Livak KJ and Schmittgen TD: Analysis of relative gene expression data using real-time quantitative PCR and the 2(-Delta Delta C(T)) method. Methods 25: 402-408, 2001.
37. Kuwabara WMT, Zhang L, Schuiki I, Curi R, Volchuk A and Alba-Loureiro TC: NADPH oxidase-dependent production of reactive oxygen species induces endoplasmatic reticulum stress in neutrophil-like HL60 cells. PLoS One 10: e0116410, 2015.
38. Guo Y, Gao F, Wang Q, Wang K, Pan S, Pan Z, Xu S, Li L and Zhao D: Differentiation of HL-60 cells in serum-free hematopoietic cell media enhances the production of neutrophil extracellular traps. Exp Ther Med 21: 353, 2021.
39. Yen MC, Yeh IJ, Liu KT, Jian SF, Lin CJ, Tsai MJ and Kuo PL: Next-generation sequencing predicts interaction network between miRNA and target genes in lipoteichoic acid-stimulated human neutrophils. Int J Mol Med 44: 1436-1446, 2019.
40. Coady TH and Lorson CL: SMN in spinal muscular atrophy and snRNP biogenesis. Wiley Interdiscip Rev RNA 2: 546-564, 2011.
41. Pennamen P, Le L, Tingaud-Sequeira A, Fiore M, Bauters A, Van Duong Béatrice N, Coste V, Bordet JC, Plaisant C, Diallo M, *et al*: BLOC1S5 pathogenic variants cause a new type of Hermansky-Pudlak syndrome. Genet Med 22: 1613-1622, 2020.
42. Blanter M, Gouwy M and Struyf S: Studying neutrophil function in vitro: Cell models and environmental factors. J Inflamm Res 14: 141-162, 2021.
43. von Aulock S, Morath S, Hareng L, Knapp S, van Kessel KP, van Strijp JA and Hartung T: Lipoteichoic acid from Staphylococcus aureus is a potent stimulus for neutrophil recruitment. Immunobiology 208: 413-422, 2003.
44. Askarian F, Wagner T, Johannessen M and Nizet V: Staphylococcus aureus modulation of innate immune responses through Toll-like (TLR), (NOD)-like (NLR) and C-type lectin (CLR) receptors. FEMS Microbiol Rev 42: 656-671, 2018.
45. Damsker JM, Hansen AM and Caspi RR: Th1 and Th17 cells: Adversaries and collaborators. Ann N Y Acad Sci 1183: 211-221, 2010.
46. Bradley LM, Dalton DK and Croft M: A direct role for IFN-gamma in regulation of Th1 cell development. J Immunol 157: 1350-1358, 1996.
47. Yoshimura T and Takahashi M: IFN-gamma-mediated survival enables human neutrophils to produce MCP-1/CCL2 in response to activation by TLR ligands. J Immunol 179: 1942-1949, 2007.
48. Donath MY, Dinarello CA and Mandrup-Poulsen T: Targeting innate immune mediators in type 1 and type 2 diabetes. Nat Rev Immunol 19: 734-746, 2019.
49. Penack O, Holler E and van den Brink MRM: Graft-versus-host disease: Regulation by microbe-associated molecules and innate immune receptors. Blood 115: 1865-1872, 2010.
50. Aguzzi A, Nuvolone M and Zhu C: The immunobiology of prion diseases. Nat Rev Immunol 13: 888-902, 2013.
51. Murphy SP, Porrett PM and Turka LA: Innate immunity in transplant tolerance and rejection. Immunol Rev 241: 39-48, 2011.
52. Ito Y and Amagai M: Controlling skin microbiome as a new bacteriotherapy for inflammatory skin diseases. Inflamm Regen 42: 26, 2022.
53. de Bont CM, Boelens WC and Pruijn GJM: NETosis, complement, and coagulation: A triangular relationship. Cell Mol Immunol 16: 19-27, 2019.
54. Ko YP, Kuipers A, Freitag CM, Jongerius I, Medina E, van Rooijen WJ, Spaan AN, van Kessel KP, Höök M and Rooijakkers SH: Phagocytosis escape by a Staphylococcus aureus protein that connects complement and coagulation proteins at the bacterial surface. PLoS Pathog 9: e1003816, 2013.

55. Mori R, Tanaka K and Shimokawa I: Identification and functional analysis of inflammation-related miRNAs in skin wound repair. Dev Growth Differ 60: 306-315, 2018.
56. Tanaka K, Kim SE, Yano H, Matsumoto G, Ohuchida R, Ishikura Y, Araki M, Araki K, Park S, Komatsu T, *et al*: MiR-142 is required for Staphylococcus aureus clearance at skin wound sites via small GTPase-mediated regulation of the neutrophil actin cytoskeleton. J Invest Dermatol 137: 931-940, 2017.
57. Zhang W, Qu X, Zhu Z, Wang L, Qi Q, Zhou P, Wang X and Li W: Inhibition of miR-139-5p by topical JTXK gel promotes healing of Staphylococcus aureus-infected skin wounds. Cells Dev 166: 203658, 2021.
58. de Kerckhove M, Tanaka K, Umehara T, Okamoto M, Kanematsu S, Hayashi H, Yano H, Nishiura S, Tooyama S, Matsubayashi Y, *et al*: Targeting miR-223 in neutrophils enhances the clearance of Staphylococcus aureus in infected wounds. EMBO Mol Med 10: e9024, 2018.